

The Orthorhombic Structure of Iron: An in Situ Study at High-Temperature and High-Pressure

D. Andrault,* G. Fiquet, M. Kunz, F. Visocekas, D. Häusermann

An in situ angle-dispersive x-ray diffraction study was undertaken of iron in a laser-heated, diamond-anvil cell up to 2375 kelvin and between 30 and 100 gigapascals in Al_2O_3 - and SiO_2 -pressure media. The resolution and reliability of diffraction peak intensities allow quantitative assessment of a structural model. The results confirm that iron undergoes a phase transformation at high pressures and temperatures. The space group is $Pbcm$ for an orthorhombic lattice, and the atomic topology is close to that of ϵ hexagonal close-packed iron.

Iron is the dominant component of Earth's core, so information on its behavior at high pressures and temperatures is necessary to understand the observed seismic structure of the core, the chemical and dynamical coupling between the core and the mantle, and Earth's magnetic field. Iron's crystallographic structure at core pressures and temperatures remains uncertain (1) because: (i) there are only a few observations because of the difficulties of obtaining results under these extreme experimental conditions and (ii) the few experiments (2–4) indicate that iron undergoes phase transformations at high pressures and temperatures, but there is disagreement about the stability field of the observed phases. In particular, the existence of a possible polymorph in the high-pressure region of the γ -phase stability field (4, 5) remains controversial.

Third-generation synchrotron radiation facilities produce intense x-ray beams comparable in size (about $10\ \mu\text{m}$) with the laser hot spots generated on DACs, allowing determination of mineral and iron properties under deep Earth conditions (5, 6). Previous synchrotron radiation experiments used energy-dispersive x-ray diffraction, which suffers from an intrinsically limited detector resolution and a poor coverage of the reciprocal space. It was not possible to extract reliable intensity information, therefore crystallographic analysis was inhibited. Angle-dispersive diffraction represents a major improvement in resolution, thus making possible investigation of subtle details of the structure of iron. Another experimental challenge is the occurrence of nonquenchable high-temperature polymorphs, emphasizing the need for re-

liable in situ diffraction experiments during laser heating in the DAC.

We used a DAC with a large optical aperture (9) mounted with diamond anvils with $300\text{-}\mu\text{m}$ culets. Rhenium gaskets were preindented to a thickness of $40\ \mu\text{m}$ and drilled to a diameter of $80\ \mu\text{m}$. As samples we used a $5\text{-}\mu\text{m}$ -thick iron foil mounted between two 15- to $20\text{-}\mu\text{m}$ -thick pure Al_2O_3 or SiO_2 polycrystalline discs. Samples were heated to 2375 K using a multimode regulated YAG laser. Because the iron samples were thinner than $5\ \mu\text{m}$ we assumed that the axial temperature gradient was negligible. This assumption is supported by the experimental evidence of diffraction peak widths during laser-heating (0.07 degrees- 2θ), which are comparable to ambient condition Si-standard pattern widths ($2\theta = 0.02^\circ$ to 0.05°). Therefore, artifacts due to pressure or tem-

perature gradients (spatial or temporal) are excluded.

Temperature measurements were achieved with an optical system designed for online measurements (7). During x-ray spectra acquisition, temperature variations were monitored and kept within 50 to 100 K. Pressures were measured at room temperature before and after laser heating, using ruby fluorescence and Al_2O_3 or SiO_2 compression curves (8).

Angle-dispersive x-ray diffraction measurements were performed on the dedicated high-pressure beamline ID30 at ESRF. An x-ray beam of wavelength $0.4245\ (1)\ \text{\AA}$ was selected from an undulator using a channel-cut Si(111) monochromator. The monochromatic beam was focused using two single-electrode bimorph mirrors to FWHM of about 15 by $8\ \mu\text{m}$ (10). This size was used to minimize the horizontal temperature gradient in the x-ray spot and avoid contamination of the recorded patterns with diffraction patterns from the gasket material. Full reciprocal angle data were collected for 5 to 10 min using image plates located 400 mm from the sample (Fig. 1). Two-dimensional patterns were integrated after geometric corrections using the program Fit2d (11).

The bottom spectrum in Fig. 2 was recorded at 44.6 GPa after an initial annealing at moderate temperature that released most of the differential stresses. All the lines of ϵ hexagonal close-packed (hcp) iron (the 100, 002, 101, and 102 reflections), as well as those of Al_2O_3 are observed. This spectrum also shows two extra features located at 1.85 and $2.03\ \text{\AA}$ that are

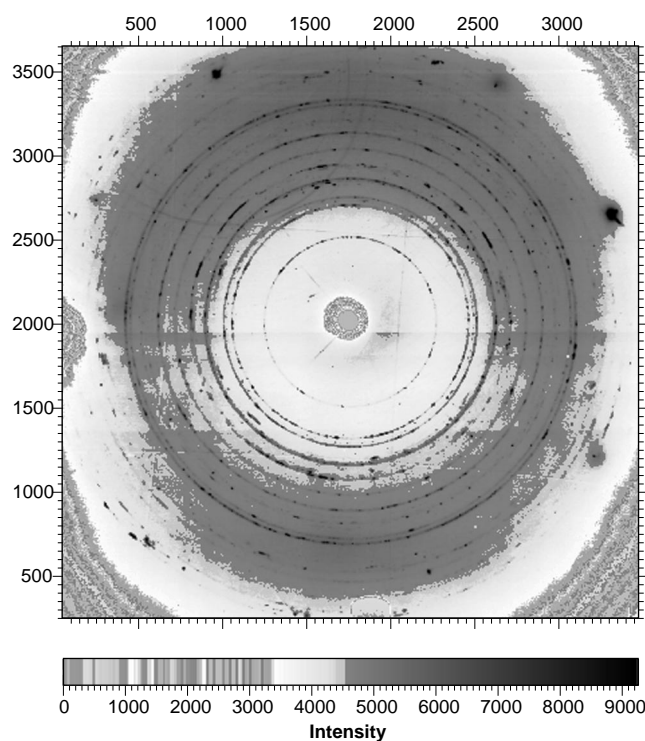


Fig. 1. Two-dimensional diffraction pattern of iron recorded on beamline ID30 at the European Synchrotron Radiation Facility during laser heating in the DAC at 44.6 GPa and 2125 (70) K.

D. Andrault and F. Visocekas, Institut de Physique du Globe, Paris 75252, France.

G. Fiquet, Ecole Normale Supérieure de Lyon, Lyon 69364, France.

M. Kunz and D. Häusermann, European Synchrotron Radiation Facility, Grenoble, 38043, France.

*To whom correspondence should be addressed. E-mail: andrault@ipgp.jussieu.fr

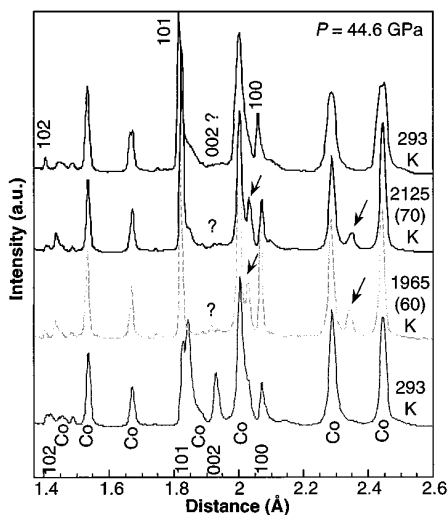


Fig. 2. Typical laser-heating sequence of angle dispersive diffraction spectra recorded at 44.6 GPa. Diffraction peaks indicated by “Co” correspond to the Al_2O_3 pressure-transmitting medium. Bottom and top spectra correspond to ϵ iron after slight laser heating and quenched spectra, respectively. New features that do not correspond to ϵ iron are clearly evident during laser heating. Among them are strong Bragg lines at 2.03 and 2.35 Å (arrows), and the absence of the hcp 002 line (question mark). All features are interpreted as the occurrence of an orthorhombic lattice for iron at high temperature. These changes cannot be preserved through quenching; a.u., arbitrary units.

not expected from a mixture of ϵ hcp iron and Al_2O_3 , but are due to initiation of the transformation of ϵ hcp iron toward a high-temperature polymorph. During laser heating up to 2125 K at 44.6 GPa, the structure of iron underwent definite changes as indicated by new diffraction lines that appeared at 1.44, 1.85, 2.03, and 2.35 Å, while the 002 ϵ hcp iron line located at 1.93 Å disappeared (Fig. 2). The new peaks do not

Table 1. Possible Bragg line indexing of the most intense diffraction lines of iron recorded at 44.6 GPa and 2125 (70) K (Fig. 2). Some experimental features cannot be explained by the occurrence of ϵ iron (indicated by +). The characteristic 002 hcp line is not observed in the experimental spectra (indicated by -). Our results are also incompatible with a δ hcp structure for iron (4, 12). Instead, we propose the occurrence of an orthorhombic lattice (Fig. 3) that explains all Bragg lines.

Exp.	Ortho.	ϵ hcp	δ hcp	
2.347	100	+	+	+
2.072	020	100	100	100
2.031	002	+	+	004
-		002	101	101
1.846	021	+	+	102
1.824	111	101	102	+
1.440	022	+	+	104
		102	104	
a (Å)	2.346	2.393	2.393	2.393
b (Å)	4.144			
c (Å)	4.063	3.845	7.690	8.126
V (Å ³)	39.500	19.068	38.137	40.299

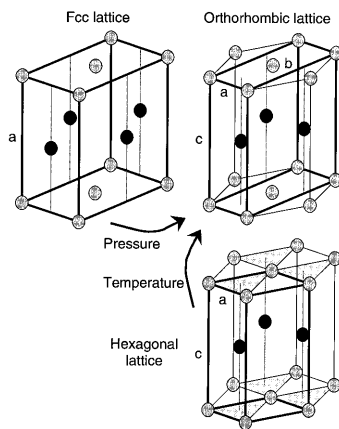


Fig. 3. A common distortion of the ϵ hcp lattice produces a doubling of the cell in the (a,b) basal plane. Doubling forms an orthorhombic unit cell, which we propose for iron at high pressures and temperatures. In this lattice, atoms are located close to face centers. The centering of the c -face is the core of the transformation between the two polymorphs. This orthorhombic lattice can also be described as a distortion of the fcc γ iron. The transformation involves the breakdown of the cubic symmetry and slight atomic displacements from the centers of the unit cell faces.

correspond to the ϵ hcp iron. They are also not compatible with γ face-centered cubic (fcc) iron found at high temperature and moderate pressure. Reaction with the pressure transmitting medium or iron oxidation is also excluded because the features are mostly unquenchable.

The occurrence of new lines at a high d_{hkl} value suggests that the size of the iron unit cell increased at high temperature. Saxena *et al.* (4, 12) proposed a doubling of the hcp unit cell along the c axis to form the δ hcp lattice with cell parameters of $a = 2.384$ and $c = 7.666$ Å at a pressure of 47 GPa. Saxena *et al.*'s δ hcp lattice could explain some of our features, but significant

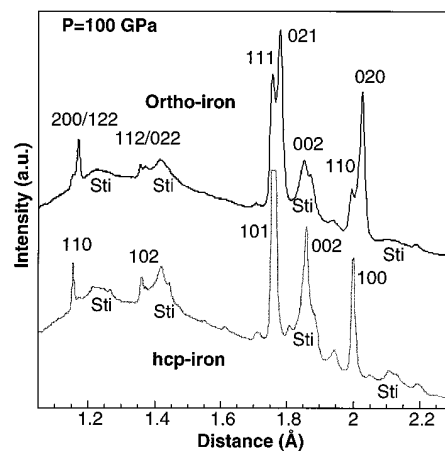


Fig. 4. Diffraction spectra of ϵ hcp and orthorhombic iron recorded at 100 GPa in an SiO_2 pressure-transmitting medium (marked as Sti). All expected diffraction lines of ϵ iron (bottom spectrum) are observed, showing that iron does not present a dominant preferential orientation in our experiments. The ϵ 101 Bragg line was truncated for reasons of clarity (intensity up to 20,000 cps). The top spectrum was recorded after laser heating at about 2300 K. It clearly shows doubling of the 100 and 101 peaks of ϵ iron, a sign of phase transformation. All diffraction features are interpreted as the occurrence of the same orthorhombic lattice as seen in Figs. 2 and 5 (see Table 2).

deviations remain uninterpreted (Table 1). We thus conclude that a δ hcp structure does not correctly fit our results.

On the other hand, all the diffraction lines observed at high temperature can be explained by a doubling of the ϵ hcp iron lattice in its basal (a,b) plane, to produce an orthorhombic unit cell. The transformation (Fig. 3) is mainly related to the deviation of the orthorhombic b/a ratio from the particular hcp value of $2\cos 30^\circ$. This orthorhombic lattice can also be derived from the γ fcc iron found at lower pressures. The intermediate structure of this new phase between γ iron and ϵ iron is a clue that explains its formation at high pressures and temperatures.

All the features of the 18-angle-dispersive spectra recorded at temperatures between 1780 and 2375 K and pressures between 30 and 60 GPa can be explained with the proposed orthorhombic lattice (Table 1). The volume of between 37.33 and 40.26 Å³ is within those of ϵ iron [36 Å³ at 50 GPa and room temperature (13)] and γ iron (40.5 Å³ after extrapolation to 35 GPa and room temperature). The cell parameters were refined as $a = 2.16$ to 2.35, $b = 4.11$ to 4.24, and $c = 4.03$ to 4.15 Å; thus, the orthorhombic iron lattice is strongly flexible (14).

To avoid any artifact related to pressure transmitting medium, we checked the occur-

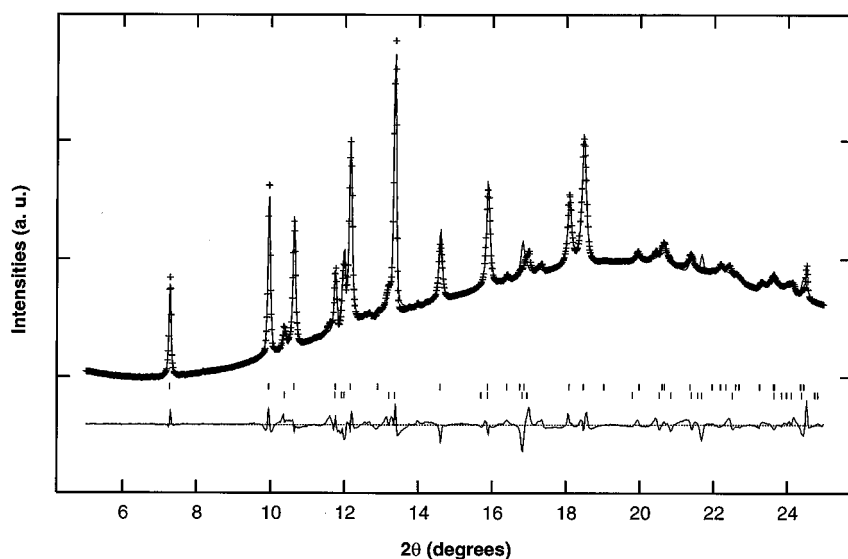


Fig. 5. Rietveld plot of spectrum recorded at 44.6 GPa and 2125 (70) K. Displayed are the observed, calculated, and difference spectra. The iron pattern (lower ticks) is associated with reflections from the Al_2O_3 pressure-transmitting medium (upper ticks).

rence of the proposed orthorhombic phase using an iron sample loaded at about 100 GPa in an SiO_2 pressure-transmitting medium (15). The SiO_2 diffraction peaks are weaker (Fig. 4) compared with that of Al_2O_3 (Fig. 2) because of the reduced thickness of the SiO_2 -iron- SiO_2 sandwich. Iron was not sufficiently insulated from the diamonds, and it was difficult to produce in situ x-ray patterns during stable laser heating.

After laser heating at about 2300 K, the diffraction pattern clearly shows a doubling of the 100 and 101 lines of the hcp lattice (Fig. 4). All the lines are explained by the same orthorhombic lattice (Table 2) we proposed for the Al_2O_3 experiments at 2125 K and 44.6 GPa (Fig. 2). At this higher pressure, the high-temperature polymorph is preserved after the quench. However, we observed rapid back-transformation to ϵ iron after a slight pressure decrease. At 100 GPa, the orthorhombic lattice is found to be about 1% denser than that of the hcp lattice, with respective values of 10.76 and $10.85 \times 10^3 \text{ kg/m}^3$.

We also double-checked our finding against a possible data contamination from the gasket signal. This was done by repeating exactly the same experiments but using W instead of Re as the gasket metal. The diffraction patterns observed during these experiments showed the same new peaks at high pressure and temperature.

We used the spectrum recorded during laser heating at $2125 \pm 70 \text{ K}$ at 44.6 GPa (Fig. 2) for a structure refinement of the iron. In order to determine possible space groups, we checked the indexed pattern for systematic absences. The absence of the 010, 001, and 011 reflections, and the pres-

ence of the 100 reflection, suggested the following space groups as candidates for the new phase: *Pccb* (54), *Pmcb* (55), *Pbcm* (57), and *Abmm* (67). We then deduced the symmetry elements for orthorhombic iron based on the assumption that its atomic arrangement represents the most symmetric distortion from that of ϵ hcp iron. This analysis yielded space group *Pbcm* (57), which we used in a subsequent LeBail refinement using the program package GSAS (16). The LeBail refinement (*Rwp* <1%) yielded orthorhombic cell parameters close to those of a pseudohexagonal unit cell. However, additional modeling

Table 2. Bragg indexing of the iron diffraction lines recorded at about 100 GPa in an SiO_2 pressure-transmitting medium (Fig. 4). Hcp iron was obtained after laser annealing at moderate temperatures (100 GPa, Annealed). Iron adopts an orthorhombic lattice after laser heating up to about 2300 K (100 GPa, quenched). This lattice perfectly explains the 10 iron diffraction lines of the spectrum; it shows the same Bragg features as at lower pressures in the Al_2O_3 pressure medium (44.6 GPa, 2125 K, Fig. 2).

Medium <i>P</i> (GPa) <i>T</i> (K)	SiO_2 100 annealed	SiO_2 100 quenched	Al_2O_3 2125
	d hkl_{hcp}	d hkl_{ortho}	Ortho.
100	2.001	100 020 110	2.288 2.027 1.996
002	1.859	002	1.857
101	1.760	021 111	1.779 1.756
102	1.361	022 112	1.372 1.357
110	1.155	122 200	1.171 1.152
<i>a</i> (Å)	2.306		2.292
<i>b</i> (Å)	2.306		4.054
<i>c</i> (Å)	3.712		3.708
<i>V</i> (Å ³)	34.189		34.451
			Ortho.
			2.347 2.072 2.031 2.031 1.846 1.824 1.440 1.440
			2.346 4.144 4.063 39.500

Table 3. Parameters related to the structural refinement of iron laser heated at 2125 (70) K at 44.6 GPa (Fig. 4). Uncertainties are given on the last significant digits in parentheses. The analysis was performed using the program package GSAS. We deduced the space group from systematic extinctions and a symmetry analysis (see text).

Space group	<i>Pbcm</i> (57)
<i>a, b, c</i> - lattice (Å)	2.3460(2), 4.1443(5), 4.0632(4)
Iron coordinates	0.220(1), 0.037(1), 1/4
No. of reflections	60 (iron + Al_2O_3)
No. of observations	1538
<i>R_p</i>	0.69%
<i>R_{wp}</i>	1.113%
<i>R</i> (<i>F</i> ²)	5.7%
X-ray wavelength	0.4245 Å

and refinements using hexagonal space groups and unit cells were not able to reproduce the observed pattern.

We then refined atomic coordinates from starting parameters obtained through the symmetry analysis described above. The refinement converged to an *R*(*F*²) of 5.7%. It also revealed a slight preferred orientation with the *c* axis parallel to the incident beam and symmetry axis of the DAC. The iron atom refined to a 12-coordinated site, similar to the iron environment in ϵ hcp iron, but distorted (Table 3 and Fig. 5). The new structure can be described as a simple shift of the hcp-AB layers relative to each other sub-parallel to (110)-hex by roughly 0.3 Å. This simple transformation mechanism, together with the high quality of the refinement supports the proposed model.

There have been several recent studies

of the high-temperature structural modifications of iron between 30 and 60 GPa. Funamori *et al.* (17) found γ iron to be stable up to 32 GPa and 1500 K. Saxena *et al.* (4, 12) suggested that iron underwent a phase transformation to β phase with δ hcp structure at 40 to 60 GPa. They recorded x-ray patterns on quenched samples previously heated with intentionally strong temperature gradients [see figure 2 in (12)]. In such an experimental procedure, samples were most likely subjected to strong stress fields that might bias structural determinations. Dubrovinsky *et al.* (18) recently provided experimental data supporting a δ hcp structure. The major evidence was the presence of 004 and 103 Bragg lines, which however disappeared with prolonged heating; thus raising the possibility that the reflections were from an unstable intermediate iron structure. Yoo *et al.* (5) recognized a metastable new polymorph at lower pressures and located it within the previously defined γ iron stability field. They did not observe a phase transformation when laser heating ϵ iron between 40 and 60 GPa. The absence of a phase transformation in this range disagrees with the other reports (2–4) and our study.

All of our spectra recorded at high-temperatures from 30 to 60 GPa and at 100 GPa correspond to the described orthorhombic lattice. The stability field of this polymorph thus appears similar to that proposed by Saxena *et al.* (4) for the β phase. We believe that the main difference between their study and our work lies in the interpretation of the diffraction patterns, and thus propose that the structure of the β

phase is the orthorhombic lattice. From our results, it appears that the stability field of γ iron should not extend much above 32 GPa, while that of β iron extends up to at least 100 GPa (Fig. 6).

REFERENCES AND NOTES

- O. L. Anderson and A. Duba, *J. Geophys. Res.*, in press.
- J. M. Brown and R. G. McQueen, *ibid.* **91**, 7485 (1986).
- R. Boehler, *Geophys. Res. Lett.* **13**, 1153 (1986); *Nature* **363**, 534 (1993).
- S. K. Saxena, G. Shen, P. Lazor, *Science* **260**, 1312 (1993); S. K. Saxena *et al.*, *ibid.* **269**, 1703 (1995).
- C. S. Yoo, J. Akella, A. J. Campbell, H. K. Mao, R. J. Hemley, *ibid.* **270**, 1473 (1995).
- G. Fiquet *et al.*, *Phys. Earth Planet. Inter.*, in press.
- See (6) for details of the experimental setup [G. Shen and P. Lazor, *J. Geophys. Res.* **100**, 17699 (1995)].
- As mentioned in previous reports [D. L. Heinz, *Geophys. Res. Lett.* **17**, 1161 (1990); see (6)], the pressure slightly increases within the laser hot spot. We estimated a correction, and we will not further discuss such effects.
- J. C. Chervin, B. Canny, P. Pruzan, *Rev. Sci. Instrum.* **66**, 2595 (1995).
- D. Häusermann and M. Hanfland, *High Press. Res.* **14**, 223 (1996).
- J. Hammersley, *ESRF publication* (1996).
- S. K. Saxena, L. S. Dubrovinsky, P. Häggkvist, *Geophys. Res. Lett.* **23**, 2441 (1996).
- H. K. Mao, Y. Wu, L. C. Chen and J. F. Shu, *J. Geophys. Res.* **95**, 21737 (1990).
- A similar flexibility was also reported for the ϵ iron lattice when coexisting with α iron [E. Huang, W. A. Basset, P. Tao, in *High-Pressure Research in Mineral Physics*, M. H. Manghni and Y. Syono, Eds. (American Geophysical Union, Washington, DC, 1987), pp. 165–172].
- The pressure is calculated from the 110 Bragg line of SiO_2 found at 2.754 Å, and according to the compression curve presented by Y. Tsuchida and T. Yagi [*Nature* **340**, 217 (1989)]. The SiO_2 diffraction features were satisfactorily reproduced using the stishovite indexing, and volume was calculated to be 38.090 Å³.
- A. LeBail, in *Accuracy in Powder Diffraction*, E. Prince and J. K. Stalick, Eds., (NIST, Maryland, 1992), p. 213; A. C. Larson and R. B. Von Dreele, *Los Alamos National Laboratory LAUR publication* (1994).
- N. Funamori, T. Yagi, T. Uchida, *Geophys. Res. Lett.* **23**, 953 (1996).
- L. S. Dubrovinsky, S. K. Saxena, P. Lazor, *ibid.* **24**, 1835 (1997).
- R. Boehler, N. Von Bargen, A. Chopelas, *J. Geophys. Res.* **95**, 21731 (1990); G. Shen, P. Lazor, S. K. Saxena, *Phys. Chem. Min.* **20**, 91 (1993).
- We thank S. Bauchau, J. Peyronneau, R. Viscoekas for experiments; F. Guyot, M. Hanfland, J. P. Poirier for discussions; C. McCammon and J. Hohl for corrections; W. A. Basset, O. L. Anderson, and anonymous reviewers for comments; and Jibidouille for graphics. This work was initiated from collaboration with P. Richet and P. Gillet and supported by Dynamique et Bilan de la Terre II.

10 June 1997; accepted 6 October 1997

Three-Dimensional Dynamic Simulation of the 1992 Landers Earthquake

K. B. Olsen,* R. Madariaga, R. J. Archuleta

The 1992 Landers, California, earthquake (magnitude 7.3) was modeled as the propagation of a spontaneous rupture controlled by a realistic prestress distribution with the use of a three-dimensional finite-difference method. The dynamic rupture reproduces the general slip pattern used to compute the initial stress distribution and generates near-fault ground motions at the surface similar to observations. The simulated rupture propagates on the fault along a complex path with highly variable speed and rise time, changing the magnitude and pattern of the stress significantly. The method provides the framework to estimate earthquake rupture parameters from recorded seismic and geodetic data.

The rupture of earthquakes and the resulting ground shaking have usually been studied from two complementary but different perspectives. The rupture is typically analyzed by seismologists interested in the initiation, propagation, and healing of earthquake ruptures using complicated models (1, 2), whereas the resulting ground shaking is generally computed in specific areas on the basis of a simple kinematic definition of

the source (3). Here, we combine the two efforts into a single integrated approach, including the computational efficiency of recent kinematic methods (4). We assume rupture on a planar, vertical fault, although it would be possible in principle to simulate more complex ruptures.

The main assumption in seismic source dynamics is that traction and slip, the relative displacement of one side of the fault with respect to the other, are related by a friction law across the fault zone. This friction law is a function of local rupture parameters including slip (D), slip rate (\dot{D}), and certain state variables (5) that describe the aging of fault contacts, fluid pressure, temperature, and several other slowly vary-

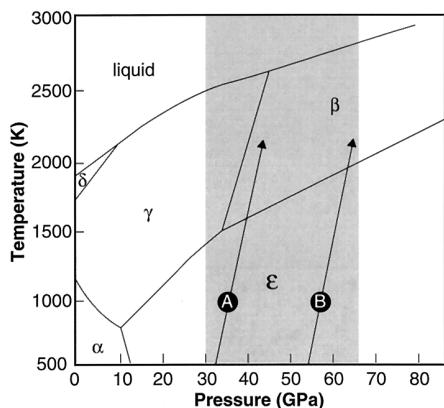


Fig. 6. Revised pressure-temperature phase diagram of iron [derived from (12)]. The A and B arrows are an estimate of the pressure-temperature path of iron during laser heating under pressure. We maintain β iron as a name for the newly determined orthorhombic structure. Melting curve was determined by Boehler *et al.* and Shen *et al.* (3, 19). Persistence of the γ phase at 32 GPa and 1500 K was indicated by in situ x-ray experiments (17).

K. B. Olsen and R. J. Archuleta, Institute for Crustal Studies, University of California, Santa Barbara, CA 93106–1100, USA.
R. Madariaga, Laboratoire de Géologie, Ecole Normale Supérieure, 24 rue Lhomond, 75231 Paris Cedex 05, France.

*To whom correspondence should be addressed.